Microseismic feasibility study: detection of small magnitude events (M_L<0.0) for mapping active faults in the Betic Cordillera (Spain)

Martin Häge and Manfred Joswig
Institute for Geophysics, Universität Stuttgart, Germany

Abstract
We present the results of the first application of the newly developed concept «Nanoseismic Monitoring» on active faults in the region close to Murcia, Spain. The aim of this microseismic feasibility study is to test if it is possible to record small magnitude events (M_L<0.0) within a short period of time with surface installations and to investigate if these events are related to the regional catalog in terms of amount of events. The seismic monitoring was performed with one small array called the Seismic Navigating System. It consists of one central three component and three one component seismometers arranged tripartitely around the central station. In the measurement period of two nights at two different sites we were able to detect 19 microearthquakes down to M_L = -2.6. The results correlate well with the frequency-magnitude distribution of the regional bulletin. This in turn will allow for estimation of monitoring rates before actual field measurements just from bulletin data. Given an activity rate of 5 to 10 events per night one may map active fault zones within just a few weeks of field campaign.

Key words *Betic Cordillera – active faults – microseismicity – Gutenberg-Richer law – Nanoseismic Monitoring*

1. Introduction

Characterizing recent seismicity and mapping active fault segments must be based on the compilation of seismological bulletins. The fundamental data collection by semi-permanent seismic networks is a time-consuming and costly task. Only a few studies deal with the investigation of small magnitude events (M_L<0.0) (*e.g.*, Abercrombie, 1995; von Seggern *et al.*, 2003; Ruiz *et al.*, 2006), whereby most researchers investigate aftershocks and not the background seismicity or use borehole sensors for event detection. Butler (2003) suggests the term «nanoearthquakes» for events with M_L<0.0.

The concept of Nanoseismic Monitoring (Joswig, 2008), a technique developed to detect and characterize small magnitude sources, is tested as a short-term alternative for semi-permanent seismic networks to reduce network recording time. It is successfully tested for On-Site-Inspections of the Preparatory Commission for the Comprehensive Nuclear-Test-Ban Treaty Organization and was applied to detect and characterize small magnitude events triggered by material impacts in sinkholes along the western Dead Sea shores (Wust-Bloch and Joswig, 2006). Nanoseismic Monitoring as a kind of seismological microscope shall finally help to shed light on small earthquake trigger mechanisms. Fault weakness can be caused by increased fluid pressure that reduces the effective normal stress (Hainzl *et al.*, 2006). In this

Mailing address: Dr. Martin Häge, Institute for Geophysics, Universität Stuttgart, Azenbergstrasse 16, 70174 Stuttgart, Germany; e-mail: haege@geophys.uni-stuttgart.de

model, stress and pore pressure redistribution after large earthquakes come along with higher permeability for fluids causing possible new nucleation points and a characteristic migration scheme (Cox, 1995; Miller *et al.*, 2004). The detection and location of small magnitude seismicity may support this model of fluid transport and a shear stress behavior driven by porosity reduction (Johnson and McEvilly, 1995; Miller *et al.*, 1996).

For the study, a seismically active section of the Betic Cordillera (near Murcia in Spain) with favorable signal-to-noise conditions was selected. Since we started to build up the system at that time one recording unit was available for field use. The small magnitude seismicity detected and partly localized by the single, small-aperture tripartite array within two successive monitoring nights, at two different sites, is compared with the regional 1984-2003 bulletin of the Instituto Geográfico National, Madrid (IGN). Brune and Allen (1967) have shown along the San Andreas Fault system that usually a two-day measurement of seismic activity is sufficient to make an approximate estimation about the local rate of microseismicity.

2. Geological and tectonic setting

The Betic Cordillera, which is situated in the southern part of Spain, is a collision zone generated by the nearby African-Eurasian plate boundary. This boundary is defined by a high seismicity which is distributed over several hundreds of kilometers (Calvert *et al.*, 2000). The area selected for the feasibility study lies within the Subbetic Zone which, together with the Prebetic Zone, represents the External Zone of the Betic Cordillera. The thickness of the crust beneath the Betic is 25-39 km (Banda *et al.*, 1993). Focal depths of regional events is restricted to the top 40 km (fig. 1) with moderate magnitudes generally less than 5.5 (Buforn *et*

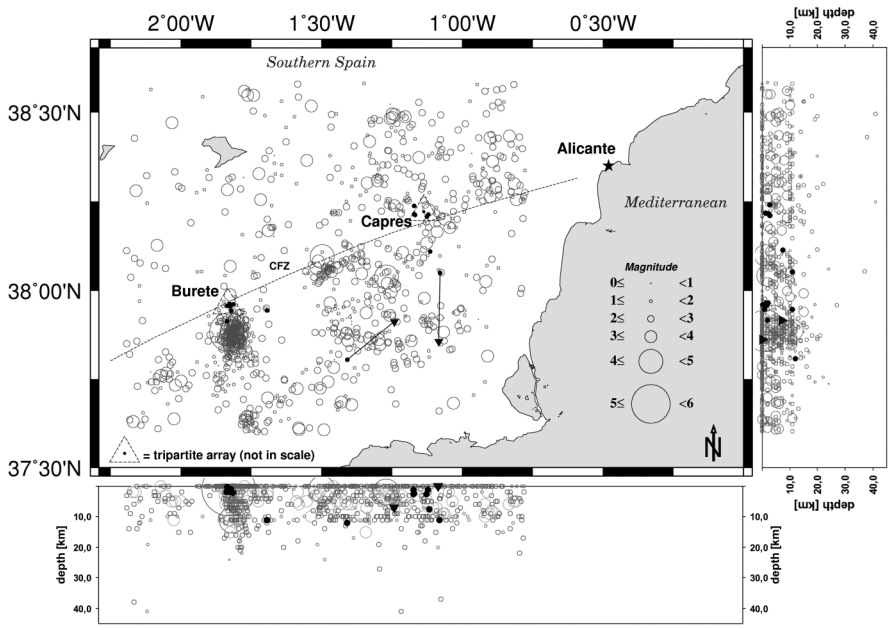

Fig. 1. Spatial distribution of 1040 earthquakes from 1984-2003 (Source: IGN, 2004). The two measuring sites (Capres and Burete) are indicated by triangles pointing up (not in scale). Our located events are marked by black dots and the two co-detected events by triangles pointing down, connected with lines. The dashed black line sketches the trace of the Crevillente Fault Zone (CFZ).

al., 2004). The shallow seismicity is associated with the dense spread of fractures in this region (Sanz de Galdeano *et al.*, 1995).

Nanoseismic Monitoring was carried out at two different locations in the vicinity of the Crevillente Fault Zone (CFZ): one near Capres, at the fringe of the Fortuna basin; the other near Burete, in the east of the Sierra de Espuna (fig. 1). The CFZ strikes NE-SW parallel to the axis of the Subbetic Zone and extends laterally over 600 km. The main activity of the CFZ was during Late Miocene (Alfaro *et al.*, 2002), and it is still active. Focal mechanisms indicate that the CFZ is a right-lateral strike slip fault which can also be observed on geological features (Buforn *et al.*, 1988). Estimates for the total displacement along the CFZ range between 75-100 km (Nieto and Rey, 2004) and 400 km (de Smet, 1984).

The Subbetic Zone consists of deposits situated far from the South Iberian Margin (Ruano *et al.*, 2004) which comprise parautochthonous to allochthonous, non-metamorphic sediments.

The main geological units in these areas beside Quaternary unconsolidated sediments and Miocene alluvial fan deposits include Triassic marls, claystones, gypsum, dolomites as well as Jurassic and Cretaceous limestones and marls. To consider potential site effects, the thickness of sediments to the top of the basement at each of the two monitoring sites has been estimated on the basis of available data and field evidence: near Capres the thickness of sediments reaches 100 m (IGN, 1972a), near Burete it is about 50 m (IGN, 1972b; Poisson and Lukowski, 1990).

3. Data acquisition and processing

Data was acquired by one Seismic Navigation System (SNS). This six-channel SNS is a portable, sparse array consisting of four short-period sensors: a central, three-component instrument and three one-component seismometers arranged as a tripartite array. High resolution and coherency of microseismic events are attained by utilizing a small aperture of 200 m and 400 Hz sampling rate. Nanoseismic Monitoring was performed at night to reduce the effect of anthropogenic noise sources. Event detection and location were carried out by SonoDet and HypoLine modules of the SparseNet software (Joswig, 1999; 2008).

Measurements were performed during four nights. Due to the first operation of the system some adaptations to the equipment had to be made in the field. Two of the four nights were successfully completed and were taken for analysis. During this period, a total of 19 seismic events in the magnitude range $-2.6 \leq M_L \leq 1.5$ could be detected and discriminated from noise bursts by sonogram analysis (Joswig, 1990) (see table I). Figure 2 shows two examples of table I, events nos. 5 and 11, demonstrating the usefulness of sonograms for event detection. Hypocentral locations could be estimated for 15 events. Four other weak events did not present clear P- and S-phase onsets. However, M_L magnitudes could be estimated for all 19 events as maximum amplitude and distance from t_s-t_p time differences could be estimated with confidence by sonogram analysis (Catalog A of table II).

The apparent velocities of most of the events, derived from array analysis, were not in accordance with much faster velocities of the standard velocity model for Spain (Dãnobeitia *et al.*, 1998). Location residuals reduced significantly using a data-adapted half-space model with velocities ranging from v_P = 1 to 5 km/s for 0.3 to 14 km depth.

Figure 1 shows the location of the 15 events (solid black dots) on the background of the regional seismicity from 1984-2003 (open gray circles). Both positions of the SNS deployments are marked with triangles pointing up (not in scale). Most of the events south of Burete are aftershocks and were generated by the 2002 Bullas (M_L = 5.0) earthquake (IGN, 2004) that occurred 607 days before our measurement. Event locations were calculated with one single array which results in a large location error of a few kilometers. Depths were estimated with the intersection of hyperboloids by t_P-t_P information. Two events were co-detected by the local network (nos. 3 and 12 in table I) which are displayed as triangles pointing down in fig. 1. For these two events, the mean horizontal location difference is about 20 km and the mean

Table I. Parameters of the recorded events.

Number	Date	Origin [UTC]	Longitude	Latitude	Depth [km]	Magnitude [M_L]
1	3-04-2004	20:45:45	-1.8359	37.9567	0.3	-2.5
2	3-04-2004	21:31:27	-	-	-	-0.8
3	3-04-2004	23:25:30	-1.4090	37.8050	12.0	1.5
4	3-04-2004	23:54:15	-1.8369	37.9136	2.0	-1.1
5	4-04-2004	1:00:58	-	-	-	-0.8
6	4-04-2004	1:17:28	-1.8267	37.9615	1.4	-1.9
7	4-04-2004	1:40:53	-1.8209	37.9430	0.9	-2.6
8	4-04-2004	1:48:20	-1.6941	37.9436	11.0	-0.3
9	4-04-2004	3:38:51	-1.8248	37.9560	1.8	-2.0
10	4-04-2004	5:05:15	-1.8135	37.9614	2.0	-2.1
11	4-04-2004	21:33:18	-1.1682	38.2121	2.4	-1.7
12	5-04-2004	0:41:02	-1.0790	38.0490	11.0	0.6
13	5-04-2004	1:46:05	-1.1147	38.1096	7.5	0.0
14	5-04-2004	2:20:08	-	-	-	-1.4
15	5-04-2004	2:34:35	-1.1714	38.2146	1.2	-1.4
16	5-04-2004	2:42:33	-1.1264	38.2077	2.7	-1.6
17	5-04-2004	2:50:22	-1.1213	38.2133	1.2	-1.5
18	5-04-2004	3:18:59	-1.1718	38.2375	2.7	-0.9
19	5-04-2004	5:34:59	-	-	-	-0.9

magnitude variation 0.4. Figure 3 plots magnitudes *versus* distances for all 19 events and the distance-correction curve used for M_L calculation fitted empirically to the data (note: slant-distance instead of epicentral distance for <10 km). Additionally, the two co-detected events are shown with triangles pointing down.

The observed detection threshold indicates that signal-to-noise conditions were better at Burete than at Capres. The overall sensitivity limit was about M_L = -1.0 at 10 km, and M_L = -2.0 at 2.5 km.

4. Characterization of regional seismicity

The 1984-2003 regional seismic catalog (IGN, 2004) was used to assess the performance of our measurement. Magnitudes of both datasets, are equivalent. By fig. 3, and as will be shown later in fig. 5, our magnitude of completeness is M_L = -1.0 in about 10 km distance. However, the analysis of regional seismicity within a 10 km radius presents several challenges.

First, the local bulletin (1984-2003) in-

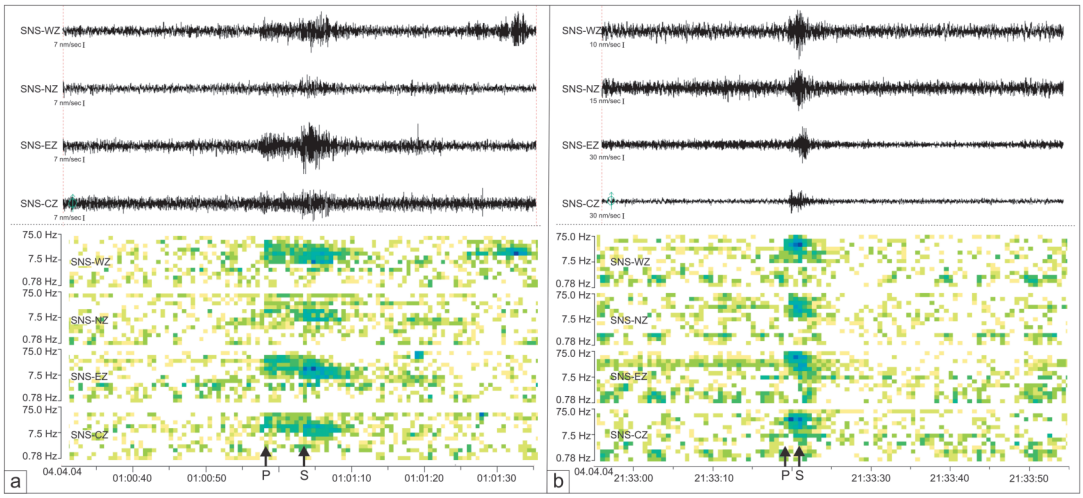

Fig. 2. Seismograms and the corresponding sonograms of the four vertical components for two events. Seismograms are filtered between 3 and 30 Hz (optimized filter setting). P and S onsets are indicated with arrows. The event in a) corresponds to no. 5, the event in b) to no. 11 in table I.

Table II. Data parameters of seismic Catalogs A, B and C. Catalog A includes 19 events recorded during this measurement campaign. Catalog B includes events within a 10 km radius of our two measurement sites in the period 1984-2003. Catalog C covers a larger area for a statistical robust b-value calculation in the period 1984-2003.

Catalog	A	B		C
Description	Nanoseismic Monitoring	Local Capres	Burete	Regional
Size of area [km^2]	630	300	300	13620
Number of events	19	34	175	1040
Max M_L	1.5	3.4	5	5
Min M_L	-2.6	1	0.4	0.4

cludes very few events whose source is located within 10 km radius of the two recording sites (Catalog B of table II). Consequently, a much larger reference area (about 13,620 km^2) with 1040 events was selected for increased statistical stability (Catalog C of table II).

Second, homogeneous seismicity in time and space is a prerequisite when comparing source regions of different size.

Artifacts like modifications in network geometry and density, station hardware and processing software result in a rather heterogeneous distribution of seismicity, both in space (fig. 1), and in time.

Figure 4 shows Catalog C of table II with 1040 events as open gray circles (right vertical axis) and the annual event frequency by the black curve (left vertical axis).

The annual event frequency and the detection level increase with time.

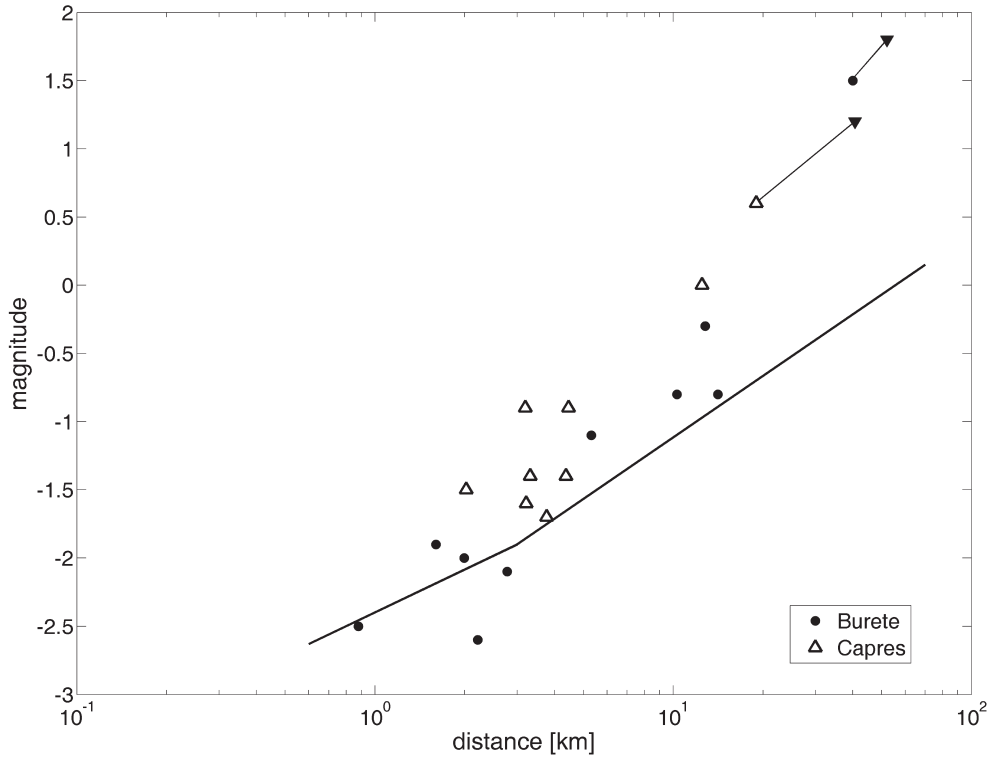

Fig. 3. Magnitude-distance relationship for the 19 events detected at Burete and at Capres as well as the distance correction for M_L. The two co-detected events are shown with triangles pointing down, linked to the corresponding events by gray lines.

Numerous investigations deal with catalog completeness and its statistical fluctuations (*e.g.*, Rydelek and Sacks, 1989; Zúñiga and Wiemer, 1999; Woessner and Wiemer, 2005).

The first change took place in 1997 when a digital recording system was installed; the second jump occurred after 2000 when another two stations (ETOB and EMUR) were added. An additional increase in number of events is caused by the aftershock activity of the 2002 Bullas $M_L = 5.0$ earthquake. Between 1984 and 1998, there is a constant magnitude of completeness (M_C) of 2.6, calculated with the entire-magnitude-range method (Woessner and Wiemer, 2005). It has decreased since 1998. Further investigations have shown that there is no catalog contamination by quarry blasts.

5. Gutenberg-Richter relationship: regional seismicity and Nanoseismic Monitoring

We make two assumptions in order to compare the Gutenberg-Richter relationship estimated from the regional seismicity (Catalog C of table II) with the same relationship based on nanoseismic data (Catalog A of table II). First, Catalog C characterizes a representative b-value for the whole region. This assumption is rooted in fig. 4 which shows an average constant seismicity without any high seismicity cycles above $M_C = 2.6$. Second, Catalog A can be obtained by concatenating the data recorded over two nights near Capres and near Burete without loss of statistical significance.

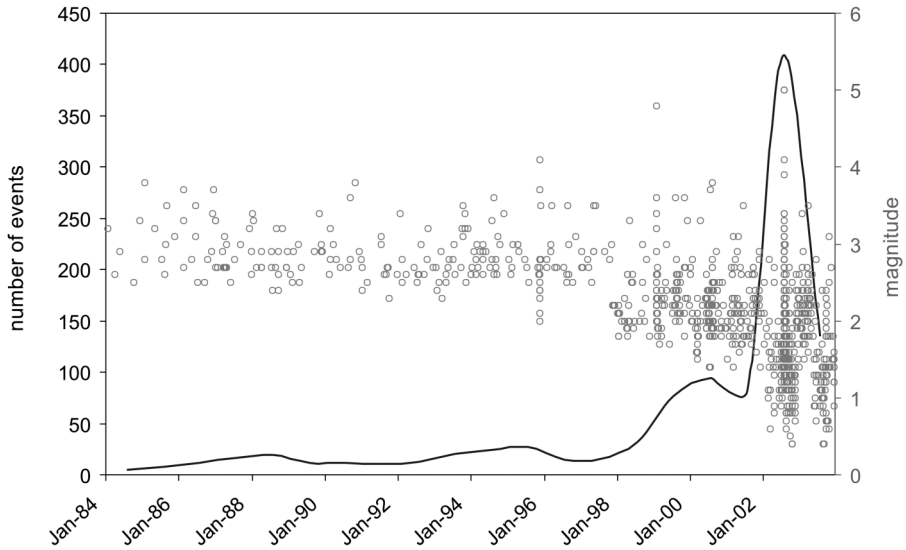

Fig. 4. Time-event (left vertical axis) and time-magnitude distribution (right vertical axis) of Catalog C of table II.

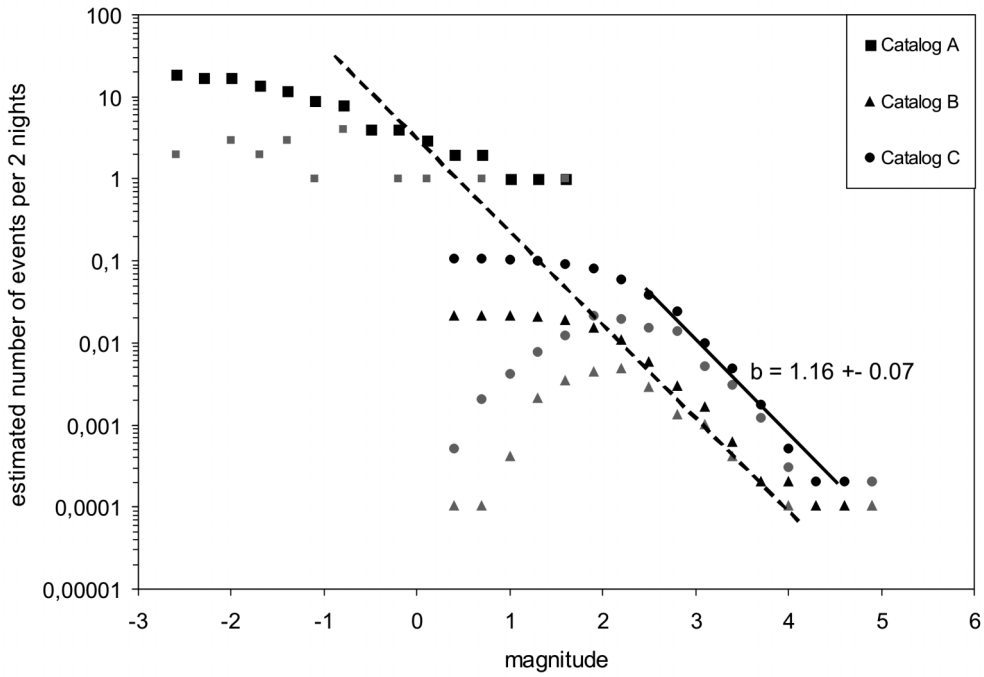

Fig. 5. Frequency-magnitude distributions of Catalogs A, B and C of table II. The cumulative distributions are marked in black, the normal distributions in grey. Note that Catalogs B and C are normalized to the measurement period of two nights. The solid black line shows the b-value for Catalog C that is applied to Catalog B (dashed black line).

Figure 5 compares the frequency-magnitude relationships for the different catalogs of table II. Note that Catalogs B and C of table II are downscaled to the measurement period of this feasibility study of two nights. Due to the small number of events of Catalogs A and B the b-value for the larger area, Catalog C, was determined and applied to our study area, Catalog A. Analyzing Catalog C (black dots) a b-value (solid black line) of 1.16±0.07 was derived according to the formula of Aki (1965) with M_C =2.6. This result corroborates the b-value of 1.1±0.1 estimated by López Casado *et al.* (1995) for magnitudes larger than 3.5 in the Murcia region between 1930-1992. In hazard assessment, the Gutenberg-Richter relation,

$$\log N = a - bM, \qquad (5.1)$$

with N the cumulative number of earthquakes of magnitude M or greater and a and b constants (Ishimoto and Iida, 1939; Gutenberg and Richter, 1944), is used to predict the frequency of occurrence of large earthquakes on the basis of smaller events. Inversely, few studies investigate the extrapolations made from the stronger to the weaker events. Studies concerned with the detection of very small earthquakes (*e.g.*, Iio, 1991; Piccinini *et al.*, 2003) or with the constancy of the b-value to lower magnitudes and self-similarity of seismic events (von Seggern *et al.*, 2003) failed to show a b-value decrease towards small magnitudes. Abercrombie and Brune (1994) verified that there was no significant decrease down to magnitude 0.0 on three major fault zones in California. Furthermore there is good agreement between b-values extrapolated from regional bulletins and those of microseismic activity (Abercrombie, 1995; 1996). Although an investigation of induced seismicity (Trifu *et al.*, 1993) showed a non-similar frequency-magnitude distribution between magnitudes -0.5 and 0.0, there is no reason why a decrease in b-value should be expected for natural seismicity at local distance.

In conclusion, the b-value of 1.16 from Catalog B was extrapolated to small magnitudes. Although it is not possible to calculate a b-value for our events and the existence of high uncertainties in the statistical estimation, *i.e.* the normalization of the frequency of events to the measurement period of two nights, the extrapolated b-value fits remarkably well with Catalog A. There might also be a slight shift in magnitudes due to the different applied velocity models which are used for location and the resulting variation in epicentral distances. However, the agreement of Catalog B with A is obvious, even with an assumed maximum magnitude deviation of 0.4. This result suggests that it might be possible to infer on the basis of bulletin data on the expected amount of events in a certain area prior to a field campaign. A similar observation was made by Brune and Allen (1967) who found out that the amount of microseismicity could be approximately predicted by extrapolation of frequency-magnitude curves from 29-year records of larger earthquakes.

6. Conclusions

In this feasibility study, the new concept of Nanoseismic Monitoring was applied to characterize small magnitude natural seismicity in the Betic Cordillera (Spain). A total of 19 events ($-2.6 \leq M_L \leq 1.5$) were recorded and detected within an observation period of two nights, indicating the high sensitivity of Nanoseismic Monitoring. The analysis of the frequency-magnitude distributions shows a good approximation between the amounts of recorded events with those extracted from local catalogs. However, it must be further proven by investigations in other geological and tectonic settings if the amount of small magnitude seismicity can be anticipated from existing catalogs by linear extrapolation.

The performance of Nanoseismic Monitoring of about M_L = -1.0 at 10 km and M_L = -2.0 at 2.5 km demonstrates its potential for a cost-effective technique for active fault mapping. Fault mapping could be realized at high resolution within weeks instead of years. Due to the use of only one small array, there is a high location error of a few kilometers. A further challenge was the discrepancy between the standard velocity model for Spain and our observations. Therefore it was not possible to identify specific fault segments. At least two small arrays

must be deployed to reach this aim. Both small arrays can be combined as a kind of network to reduce the azimuthal gap and hence to increase the location accuracy. Cross bearing and the intersection of two t_s-t_p circles provide additional location constraints and support the determination of an appropriate velocity model. It can then be tested if relative location methods might be applicable for further improvement of the location results.

Acknowledgments

The authors are grateful to the Instituto Geográfico National, Madrid, Spain, especially to Arancha Izquierdo Álvarez and Resurrección Antón for the allocation of the regional bulletin data used in this work and for their kindly support. Hillel Wust-Bloch suggested many improvements of the manuscript. The map in fig. 1 was partly created using GMT software (Wessel and Smith, 1991).

REFERENCES

ABERCROMBIE, R.E. and J.N. BRUNE (1994): Evidence for a constant b-value above magnitude 0 in the southern San Andreas, San Jacinto and San Miguel fault zones, and at the Long Valley caldera, California, *Geophys. Res. Lett.*, **21** (15), 1647-1650.

ABERCROMBIE, R.E. (1995): Earthquake source scaling relationships from -1 to 5 Ml using seismograms recorded at 2.5-km depth, *J. Geophys. Res.*, **100** (B12), 24,015-24,036.

ABERCROMBIE, R.E. (1996): The magnitude-frequency distribution of earthquakes recorded with deep seismometers at Cajon Pass, southern California*, Tectonophys.*, **261**, 1-7.

AKI, K. (1965): Maximum likelihood estimate of b in the formula log N = a – bM and its confidence limits, *Bull. Earth. Res. Inst. Tokyo Univ.*, **43**, 237-239.

ALFARO, P., J. DELGADO, A. ESTÉVEZ, J.M. SORIA and A. YÉBENES (2002): Onshore and offshore compressional tectonics in the eastern Betic Cordillera (SE Spain), *Mar. Geol.*, **186**, 337-349.

BANDA, E., J. GALLART, V. GARCÍA-DUEÑAS, J.J. DAÑOBEITIA and J. MAKRIS (1993): Lateral variation of the crust in the Iberian peninsula: new evidence from the Betic Cordillera, *Tectonophys.*, **221**, 53-66.

BRUNE, J.N. and C.R. ALLEN (1967): A micro-earthquake survey of the San Andreas Fault system in Southern California, *Bull. Seismol. Soc. Am.*, **57** (2), 277-296.

BUFORN, E., A. UDÍAS and J. MEZCUA (1988): Seismicity and focal mechanisms in South Spain, *Bull. Seismol. Soc. Am.*, **78** (6), 2008-2024.

BUFORN, E., M. BEZZEGHOUD, A. UDÍAS and C. PRO (2004): Seismic Sources on the Iberia-African Plate Boundary and their Tectonic Implications, *Pure Appl. Geophys.*, **161**, 623-646, doi:10.1007/s00024-003-2466-1.

BUTLER, R. (2003): The Hawaii-2 observatory: observation of nanoearthquakes, *Seism. Res. Lett.*, **74** (3), 290-297.

CALVERT, A., E. SANDVOL, D. SEBER, M. BARAZANGI, S. ROECKER, T. MOURABIT, F. VIDAL, G. ALGUACIL and N. JABOUR (2000): Geodynamic evolution of the lithosphere and upper mantle beneath the Alboran region of the western Mediterranean: Constraints from travel time tomography, *J. Geophys. Res.*, **105** (B5), 10,871-10,898.

COX, S.F. (1995): Faulting processes at high fluid pressure: An example of fault valve behavior from the Wattle Gully Fault, Victoria, Australia, *J. Geophys. Res.*, **100** (B7), 12,841-12,859.

DÃNOBEITIA, J.J., V. SALLARÈS and J. GALLART (1998): Local earthquakes seismic tomography in the Betic Cordillera (southern Spain), *Earth Planet. Sci. Lett.*, **160**, 225-239.

DE SMET, M.E.M. (1984): *Investigations of the Crevillente Fault Zone and its Role in the Tectogenesis of the Betic Cordilleras, Southern Spain,* (PhD Thesis, Free Univ. Press, Amsterdam).

GUTENBERG, B. and C.F. RICHTER (1944): Frequency of earthquakes in California, *Bull. Seismol. Soc. Am.*, **34**, 185-188.

HAINZL, S., T. KRAFT, J. WASSERMANN, H. IGEL and E. SCHMEDES (2006): Evidence for rainfall-triggered earthquake activity, *Geophys. Res. Lett.*, **33**, L19303, doi:10.1029/2006Gl027642.

IGN (1972a): *Mapa Geologico de España, escala 1:50.000 - Fortuna*, (Instituto Geográfico National, Madrid. Spain).

IGN (1972b): *Mapa Geologico de España, escala 1:50.000 - Coy*, (Instituto Geográfico National, Madrid, Spain).

IGN (2004): *Seismicity Data File of the Instituto Geográfico National*, (Madrid Spain).

IIO, Y. (1991): Minimum size of earthquakes and minimum value of dynamic rupture velocity, *Tectonophys.*, **197**, 19-25.

ISHIMOTO, M. and K. IIDA (1939): Observation of earthquakes registered with the microseismograph constructed recently, *Bull. Earthq. Res. Inst.*, (University of Tokyo), **17**, 443-478.

JOHNSON, P.A. and T.V. MCEVILLY (1995): Parkfield seismicity: Fluid-driven?, *J. Geophys. Res.*, **100** (B7), 12,937-12,950.

JOSWIG, M. (1990): Pattern recognition for earthquake detection, *Bull. Seismol. Soc. Am.*, **80** (1), 170-186.

JOSWIG, M. (1999): Automated processing of seismograms by SparseNet, *Seism. Res. Lett.*, **70**, 705-711.

JOSWIG, M. (2008): Nanoseismic monitoring fills the gap between microseismic networks and passive seismic, *First break*, **26**, 81-88.

LÓPEZ CASADO, C., C. SANZ DE GALDEANO, J. DELGADO and M.A. PEINADO (1995): The b parameter in the Betic Cordillera, Rif and nearby sectors. Relations with the tectonics of the region, *Tectonophys.*, **248**, 277-292.

MILLER, S.A., A. NUR and D.L. OLGAARD (1996): Earthquakes as a coupled shear stress – high pore pressure dynamical system, *Geophys. Res. Lett.*, **23** (2), 197-200.

MILLER, S.A., C. COLLETTINI, L. CHIARALUCE, M. COCCO, M. BARCHI and B.J.P. KAUS (2004): Aftershocks driven by a high-pressure CO_2 source at depth, *Nature*, **427**, 724-727.

NIETO, L.M. and J. REY (2004): Magnitude of lateral displacement on the Crevillente Fault Zone (Betic Cordillera, SE Spain): stratigraphical and sedimentological considerations, *Geol. J.*, **39**, 95-110.

PICCININI, D., M. CATTANEO, C. CHIARABBA, L. CHIARALUCE, M. DE MARTIN, M. DI BONA, M. MORETTI, G. SELVAGGI, P. AUGLIERA, D. SPALLAROSSA, G. FERRETTI, A. MICHELINI, A. GOVONI, P. DI BARTOLOMEO, M. ROMANELLI and J. FABBRI (2003): A microseismic study in a low seismicity area of Italy: the Città di Castello 2000-2001 experiment, *Ann. Geophys.*, **46** (6), 1315-1324.

POISSON, A. and P. LUKOWSKI (1990): The Fortuna Basin: a piggiback basin in the Eastern Betic Cordilleras (SE Spain), *Ann. Tect.*, **4** (1), 52-67.

RUANO, P., J. GALINDO-ZALDÍVAR and A. JABALOY (2004): Recent tectonic structures in a transect of the Central Betic Cordillera, *Pure Appl. Geophys.*, **161**, 541-563, doi:10.1007/s00024-003-2462-5.

RUIZ, M., J. DÍAZ, J. GALLART, J.A. PULGAR, J.M. GONZÁLEZ-CORTINA and C. LÓPEZ (2006): Seismotectonic constraints at the western edge of the Pyrenees: aftershock series monitoring of the 2002 February 21, 4.1 Lg earthquake, *Geophys. J. Int.*, **166**, 238-252.

RYDELEK, P.A. and I.S. SACKS (1989): Testing the completeness of earthquake catalogues and the hypothesis of self-similarity, *Nature*, **337**, 251-253.

SANZ DE GALDEANO, C., C. LÓPEZ CASADO, J. DELGADO and M.A. PEINADO (1995): Shallow seismicity and active faults in the Betic Cordillera. A preliminary approach to seismic sources associated with specific faults, *Tectonophys.*, **248**, 293-302.

TRIFU, C.-I., T.I. URBANCIC and R.P. YOUNG (1993): Non-similar frequency-magnitude distribution for M<1 seismicity, *Geophys. Res. Lett.*, **20** (6), 427-430.

VON SEGGERN, D.H., J.N. BRUNE, K.D. SMITH and A. ABURTO (2003): Linearity of the earthquake recurrence curve to M<-1 from Little Skull Mountain aftershocks in southern Nevada, *Bull. Seismol. Soc. Am*, **93** (6), 2493-2501.

WESSEL, P. and W.H.F. SMITH (1991): Free software helps map and display data, *Eos Trans. AGU*, **72** (41), 441.

WOESSNER, J. and S. WIEMER (2005): Assessing the quality of earthquake catalogs: estimating the magnitude of completeness and its uncertainty, *Bull. Seismol. Soc. Am.*, **95** (2), 684-698.

WUST-BLOCH, G.H. and M. JOSWIG (2006): Pre-collapse identification of sinkholes in unconsolidated media at the Dead Sea area by "nanoseismic monitoring" (graphical jackknife-location of weak sources by few, low-SNR records), *Geophys. J. Int.*, **167**, 1220-1232, doi:10.1111/j.1365-246X.2006.03083.x.

ZÚÑIGA, F.R. and S. WIEMER (1999): Seismicity patterns: are they always related to natural causes?, *Pure Appl. Geophys.*, **155**, 713-726, doi:10.1007/s000240050285.

(received August 15, 2008;
accepted December 11, 2008)